JOURNAL OF AIRCRAFT
Vol. 41, No. 5, September–October 2004

First Look into Effects of Discrete Midspan Vortex Injection on Wing Performance

Vojin R. Nikolic*
Minnesota State University Mankato, Minnesota 56001
and
Eric J. Jumper†
University of Notre Dame, Notre Dame, Indiana 46556

The effects of midspan discrete vortex injection on the performance of a rectangular wing model were studied in a wind tunnel. Based on this preliminary study, discrete vortex injection, while affecting the wing lift and drag, does not degrade its overall performance to any significant degree. This is particularly so in the high-angle-of-attack range where use of vortex injection for wake turbulence alleviation had been proposed. The investigation confirms and expands previously reported, computationally determined results. This study was of a limited scope; additional aspects of discrete vortex injection warrant investigation.

Nomenclature

b	=	wing model span, mm (in.)
C_D	=	wing drag coefficient
C_L	=	wing lift coefficient
c	=	wing model chord, mm (in.)
q	=	dynamic pressure of the flow, $\frac{1}{2}\rho V^2$, kPa (psf)
S	=	wing reference area, m^2 (ft^2)
s	=	wing semispan, mm (in.)
V	=	airflow speed, m/s (fps)
x, y, z	=	aerodynamic axes
α	=	angle of attack, deg

Subscripts

F	=	fin (delta wing)
W	=	main wing
0	=	zero lift condition

Introduction

WHEN the problem of wing-generated vortical wakes was studied, a new idea for trailing vortex attenuation consisting of instigating onset of a Crow-like instability mode into the vortex pair by steady injection of a pair of discrete midspan originated vortices was proposed by Nikolic and Jumper[1] and Nikolic.[2] These injected vortices then entrain a portion of the trailing vorticity in their vicinity to form a pair of secondary vortices. The rest of the wing trailing vorticity is rolled up into two primary vortices. These two pairs of vortices then interact in the near- to far-field region of the wake flowfield. For certain combinations of strength and location of injected vorticity, the primary vortex pair develops a sinusoidal type of instability of the Crow type, which leads rapidly to a breakup of the highly organized vortex flow characteristic of wing wake vortices, thus, diminishing the hazard to any following aircraft that may inadvertently encounter the vortex. The extensive computational studies in Refs. 1 and 2 have indicated that by injecting discrete vortices of moderate strength it is possible to bring about the instability onset and vortex breakup.

In the past, there have been several other vortex attenuation schemes proposed that were capable of significantly reducing the trailing vortex hazard; however, the prohibitively high performance degradations that they were causing to the wake generating airplane prevented their use.[3] In Refs. 1 and 2 attempts are reported to assess computationally the effects that the vortex injection would exhibit on the wing aerodynamic performance. It was shown that this type of vortex injection would not produce any significant performance degradation to the wing/airplane. Because the computational work could only include the effects on wing's lift and induced drag, this conclusion remained to be confirmed by experiments that would also include the wing zero lift drag. The study reported here is an attempt to accomplish that goal. The second motivation for this study was as follows. In the course of the studies reported in Refs. 1 and 2, Batill suggested (in private communications) exploring the possible effects that the injection of midspan vortices might have on the wing-bound vortex. Namely, he raised the question whether the added injected vortices, which join the wing trailing vortex filament system, will have to be continued across the wing as predicted by the Helmhotz vortex laws. If so, he suggested there should be an increase of the wing-bound vortex and, thus, lift. It is to investigate this possibility of injected vortices acting as a kind of a "vortex flap" that has also been attempted to a limited extent in the present study.

The idea of vortex injection for wake vortex attenuation was first proposed and studied experimentally by Rossow.[4] Among other devices, he employed vertically mounted lifting surfaces on top of the main wing to inject additional vortices into the wing wake flow, that is, he basically added the trailing vortices of the two small vertical wings to the wake flow of the main wing. He found considerable alleviation of the vortex problem when the vertical wings were located around midspanwise locations. Rossow attributed this alleviation to the more diffuse structure of the vortex wake brought about by the vortex injection. More diffuse wakes result in less tightly rolled up vortices and, thus, a lesser hazard to a following airplane in terms of the adverse overturning, or rolling moments. In Refs. 1 and 2 very similar results were reported from the analytical/computational studies, except that the explanation which was offered for this attenuation was based on instability considerations.

Experimental Setup

Next the wing model and wind tunnel are described. The main wing model for this study had a NACA 4412 airfoil, a chord of 99.6 mm (3.92 in.), and a span of 161.5 mm (6.36 in.), thus yielding an aspect ratio of 1.62. At the start of the investigation, a different

Received 15 July 2003; revision received 8 November 2003; accepted for publication 23 November 2003.

*Professor, Department of Mechanical Engineering. Senior Member AIAA.

†Professor, Department of Aerospace and Mechanical Engineering. Associate Fellow AIAA.

Fig. 1 View of the wind tunnel.

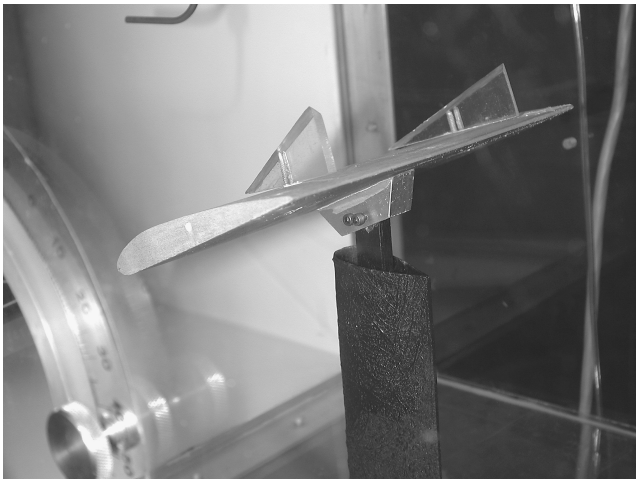

Fig. 2 Model installed in the test section.

wing model having the same airfoil, that is, NACA 4412, with a chord of 101.6 mm (4.0 in.), and a span of 300.7 mm (11.84 in.), thus, an aspect ratio of 2.96, was used to compare data from the tunnel with available published results. The span of this model closely matched the width of the wind-tunnel test section, 304.8 mm (12 in.) and, thus, simulated the two-dimensional flow conditions for comparison purposes. The wind tunnel used was designed and constructed by the Engineering Laboratory Design (ELD), Inc., of Lake City, Minnesota, ELD-402B model. The tunnel is an open-circuit type and capable of producing flow speeds of up 45.7 m/s (150 fps) and has a test section 304.8 by 304.8 mm (12 by 12 in.) Thus, the Reynolds number based on the wing chord of 101.6 mm (4.0 in.) was 0.25×10^6. A view of the tunnel is shown in Fig. 1. A strut assembly (the strut inside a streamlined shroud) connects a model with a dynamometer comprising three differential variable transducers for dynamic pressure, lift, and drag display. Angle of attack is adjusted by rotating the model attachment bracket relative to the strut and the test section (Fig. 2) and then by visually inspecting and matching the position of the airfoil section contour on a test section plug relative to the model. This procedure, although time consuming, is considered quite satisfactory in terms of its accuracy. (The uncertainties of the variables involved in this investigation will be addressed in a later section.) The airflow speed is controlled via a frequency controller of type TOSVERT-130HI Transistor Inverter by Toshiba/Houston. At the start of the investigation, the dynamic pressure component of the tunnel instrumentation was replaced by a membrane-type manometer by Magnehelic, Model 2000, having a range of 0–1.5 kPa (31.33 psf). A static pressure signal as taken at the test section floor was connected to one port of the manometer, and a total pressure input as sensed at the start of the test section away from the wall was applied to the other. Thus, the monometer directly gave the dynamic pressure of the flow. The hydrostatic pressure component due to the elevation difference of about 254 mm (10 in.) of air between the static and total pressure sensing points was considered negligible and was not included in the study. The maximum dynamic pressure attainable with this model is about 3-in. H_2O, or 0.75 kPa (15.66 psf); thus, this particular manometer was well suited for this application. Next the manometer was compared with a water column type manometer by Dwyer Instruments, Model 424, and a difference of +2.5% found at the operating pressure of 0.625 kPa (13.06 psf). The Magnehelic manometer gave consistent and repeatable readings.

The first wing model used in the study, the one with an aspect ratio of 2.96, was tested over a range of angles of attack of −5–20 deg. Also, lower negative values of α, down to −20 deg, were run; however, the tunnel was not capable of producing usable results at these test conditions. This was attributed to the increased blockage of the test section flow area at these flow conditions. In addition, it was found that when set at $\alpha = -9$ deg the model consistently underwent very violent oscillations. This resonance phenomenon is explained by the specific interaction between the flow and the model for this angle of attack; the same model behaved quite normally at both −8 and −10 deg. Therefore, the angle-of-attack range for this study was limited to −5–20 deg. This range covers virtually all of the wing's angles of attack having any practical significance. When within this range, the results compared favorably with those by Abbott and Doenhoff,[5] with the differences in the Reynolds numbers involved kept in mind. Thus, it was concluded that the tunnel was capable of producing useful data for this preliminary type of study.

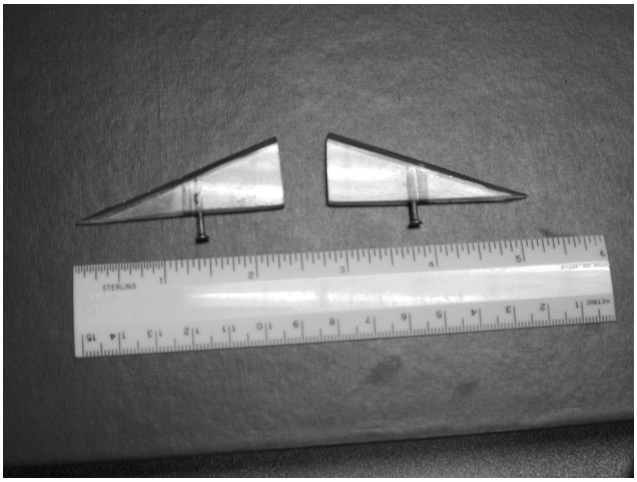

Fig. 3 Delta fins used for vortex injection.

The wing model used for the vortex injection study is shown in Fig. 2. The base wing was modified by the addition of two vertically mounted fins consisting of basically two small delta wings machined from 3.2-mm- (1/8-in.-) thick Plexiglas® and having a leading-edge sweep angle of 70 deg, root chord of 58.4 mm (2.30 in.), and semispan of 21.6 mm (0.85 in.). Thus, the aspect ratio of the fins was 1.48, and their reference area was 1261.3 mm^2 (1.955 $in.^2$), or 7.85% of the main wing area. The delta fins are shown in Fig. 3. The leading edges of the fins are beveled at 45 deg throughout the complete thickness. With a sharp leading edge, this fin was expected to act as an effective device for vortex injection in the vicinity of the main wing. The fins were attached to the main wing via pivot points located at 66.33% of the wing chord and 59.83% of the fin chord. Three values for the angle of attack of the fins, 5, 10, and 15 deg, were included in the study, but the bulk of the tests were done at $\alpha_F = 10$ deg (discussed later). Figure 2 shows the wing model with the fins attached at spanwise locations of 60% and $\alpha_F = 10$ deg.

In this study, fin angles of attack producing fin-generated vortices having the same sense of rotation as the main wing trailing vortices, or corotating vortices, are denoted as positive α_F. Only two spanwise locations, $y = \pm 0.5s$ and $y = \pm 0.6s$, referred to as $0.5b$ and $0.6b$ spans, respectively, were used. These spanwise coordinates represent the lower and upper bound, respectively, of the spanwise

station range for which it was shown that injection of discrete vortices of moderate strength would lead to an accelerated onset of sinusoidal instability of the wing trailing vortex pair.[1,2]

Discussion of Results

First a series of tests on the longer wing model, the one with an aspect ratio of 2.96 as describe earlier, were conducted. The experiments produced data points of remarkable repeatability. The C_L vs α curve, however, was consistently overestimating what would be expected based on results of Ref. 5 with the lower values of the Reynolds numbers involved in this investigation kept in mind. The tunnel is capable of producing a Reynolds number of 0.25×10^6 based on the 101.6-mm (4-in.) chord. With this model size, the corresponding airflow velocity, however, yields a lift force in excess of 35.6 N (8 lb), which is the upper limit for reliable indication by the dynamometer as recommended by the tunnel manufacturer. Therefore, the Reynolds number for this part of the investigation was lowered and kept constant at 0.225×10^6. The lift curve maintained the right constant slope in the below-the-stall region, although the lift coefficient values were somewhat larger than those of Ref. 5. After this unexpected result persevered through several series of tests with the tunnel being carefully recalibrated for each series, an explanation for it was systematically sought. First the difference was suspected to be caused by a larger effective Reynolds. The manufacturer, however, provided a turbulence level for the tunnel of only 0.25%, which corresponds to a turbulence factor of 1.2 and an effective Reynolds number of 0.27×10^6 based on results in Ref. 6. In the end, it was suspected that the relatively large trapezoidal mounting bracket identical to the one shown in Fig. 2 was generating some lift and, thus, was responsible for this result. Next, a similar wing model having the same span and chord dimensions and a NACA 0012 airfoil was tested, and the tests showed a nonzero lift coefficient (0.144) at a zero angle of attack for this symmetric airfoil. This was attributed to the contribution by the bracket, and because the two models had identical brackets, it seemed logical to subtract this same value from the NACA 4412 wing model data. The resulting value was in excellent agreement with the data published in Ref. 5.

The C_D vs α curve exhibited similarly noticeable differences with that of Ref. 5. For example, the experiments overestimated the drag coefficient at the zero lift condition by about 0.010 in C_D. At the dynamic pressure of 0.625 kPa (13.06 lb/ft^2), this translates into a drag force difference of 0.19 N (0.0435 lb). In an attempt to explain this difference, the tunnel was run with the strut only, that is, no model attached, and a drag force of 0.15 N (0.034 lb) was measured. The difference of $0.0435 - 0.034 = 0.0095$ lb, or 27.9% of the strut drag, was attributed to the presence of the sizeable bracket mentioned earlier and shown in Fig. 2. It was reasoned that the bracket with its significant frontal area and lateral areas and various sharp edges could easily account for between one-fourth and one-third of the drag of the longer strut enclosed in a streamlined shroud.

Based on this analysis, it was concluded that this experimental setup could be used for a preliminary investigation of this type. Also, the differences between various configurations rather than the absolute values of the coefficients are of primary interest in this study.

Next in the main part of the investigation, the shorter wing was tested clean and with the fins added on the top surface of the wing at different spanwise locations y_F and at angles of attack of the fins, α_F. As mentioned earlier, it was found by Rossow[4] that when discrete vortices were injected around the 50% span point they produced significant reductions in the trailing vortex hazard as measured by the coefficient of the rolling moment imposed on the following airplane. The present authors also investigated use of vortex injection for trailing vortex alleviation via instability acceleration, and in Refs. 1 and 2 it was reported that such discrete vortices when injected at spanwise locations between $0.5s$ and $0.6s$ brought about accelerated onset of sinusoidal instability of the trailing vortex pair. In the analytical and computational work reported in Refs. 1 and 2, the effects of this injection on the performance of the wake generating wing were also addressed to a limited extent. However, because of the nature of the method used (inviscid, point vortex method), only the induced component of the airplane drag could be addressed.

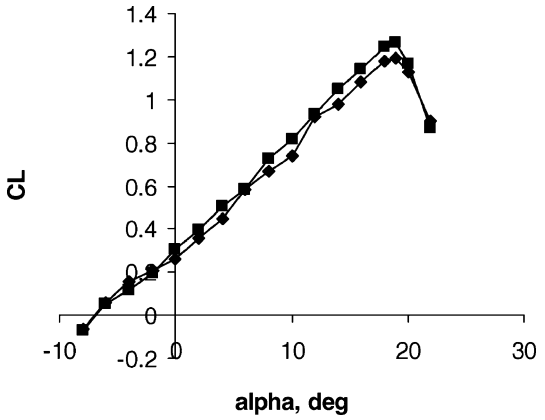

Fig. 4 Effects of vortex injection on C_L: ◆, clean wing and ■, wing with fins at $0.6b$ and 10 deg.

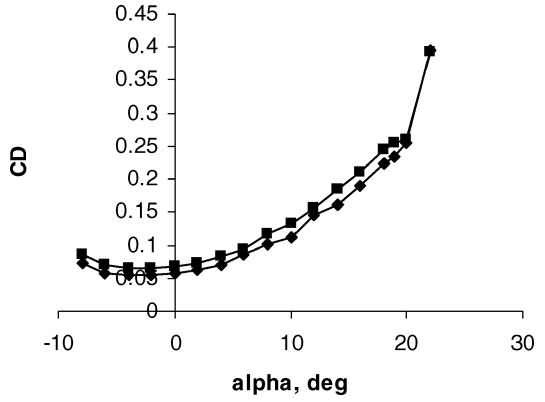

Fig. 5 Effect of vortex injection on C_D: ◆, clean wing and ■, wing with fins at $0.6b$ and 10 deg.

Figure 4 shows the lift coefficient vs angle-of-attack curves for the clean wing and the wing with the fins attached on the top surface of the wing at the locations corresponding to $y_F = \pm 0.6s$. For this series of runs, the fins were oriented at $\alpha_F = 10$ deg relative to the freestream direction. It is seen that the injected vortices consistently produced additional lift on the main wing throughout most of the angle of attack range. This lift enhancement is particularly noticeable in the range of α between 12 and 18 deg, which is exactly the range within which the fins would be deployed for trailing vortex attenuation after takeoff and on final approach for landing. A persistent lift coefficient enhancement between 5.6 and 6.0% was found for the α-range between 16 and 19 degrees. The largest lift increase of 7.5% was found at $\alpha = 14$ deg. Also note that the slope of the C_L vs α line increased by the addition of the fins. This is consistent with the fact that adding the fins, which in addition to injecting vortices act as aerodynamic fences, increases the effective aspect ratio of the main wing and, thus, the slope of this line. Note that at very high angles of attack, above 20 deg, the effects of the fins diminishes and altogether disappears at 22 deg. This is due to the massive flow separation that was observed at these poststall conditions. Figure 5 shows the drag coefficient changes due to the addition of the fins for the same fin setting. A fairly constant increase in drag coefficient on the order of 8–10% is observed over most of the range of angles of attack of interest. This drag increase is due to the increased minimum drag. At higher angles of attack, where induced drag becomes the predominant drag component, the increase in drag gradually diminishes, and at $\alpha = 22$ deg the two drag curves coincide. Note that the fins, while they are adding some drag, are also producing additional lift, which would have to be provided by deflecting flaps and other high-lift devices, which could produce even larger drag increases. Figure 6 shows the changes in the aerodynamic efficiency of the wing, the C_L/C_D curve. Although there is a drop in the wing aerodynamic efficiency over most of the angle-of-attack range, it basically remains the same in the high-angle-of-attack range.

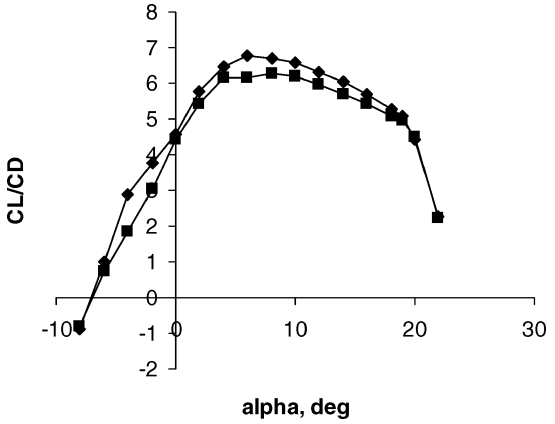

Fig. 6 Effect of vortex injection on C_L/C_D: ◆, clean wing and ■, wing with fins at 0.6*b* and 10 deg.

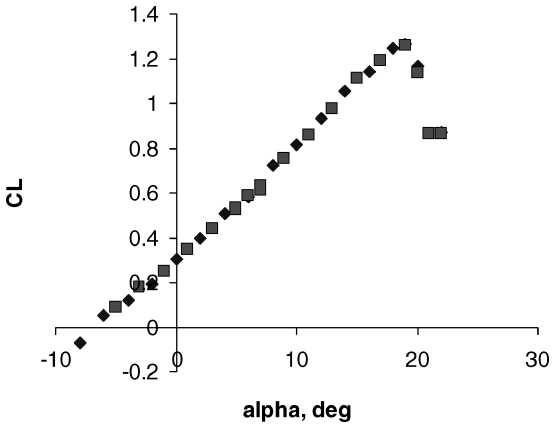

Fig. 7a Lift coefficient, fins on top at 0.6*b* and 10 deg: ◆, baseline, and ■, additional data points.

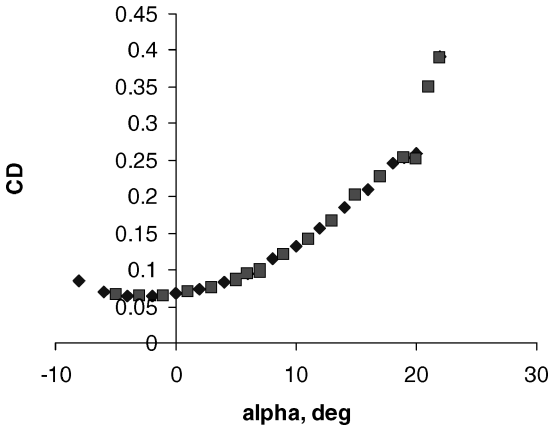

Fig. 7b Drag coefficient, fins on top at 0.6*b* and 10 deg: ◆, baseline, and ■, additional data points.

The delta fins used here modify the flow pattern around the main wing because of the following three mechanisms. First, sharp-edged highly swept delta wings are capable of generating strong leading-edge vortices, which contribute a significant portion of the lift force. These vortices flowing over the top surface of the main wing further increase the flow velocity there and, thus, generate additional lift. Second, the fins act as fences, preventing the flow in the spanwise direction. This improves the efficiency of the wing through the increased effective aspect ratio. Third, because of their orientation, the fins act as a diffuser and, thus, decrease the adverse pressure gradient on the top surface of the wing, which might be helpful from the flow separation point of view. Also, for certain angles of attack, it is possible that the fin-generated vortices will propagate close to the wing top surface and energize the flow, thus, further postponing separation. Additional studies including flow visualization are necessary to understand the nature of the flow interactions taking place fully.

To examine the level of repeatability of the tunnel data and to provide additional data, 19 data points, that is, 19 values of α, were tested on two days, after recalibrating the tunnel each time. Out of the 19 points, four α, 6, 19, 20, and 22 deg, were repeated from the first series of tests, the baseline 4 and 15 new values that were added. These new α values included the following: -5, -3, -1, 1, 3, 5 (two separate times), 7 (two separate times), 9, 11, 13, 15, 17, and 21 deg. The results of these tests are shown in Figs. 7a–7c. Note that these additional data points are in very good agreement with the data points from the first baseline series. The data point at $\alpha = 21$ deg, however, did not follow the overall trend and was off. The points at 6, 19, and 22 deg coincided with the baseline data.

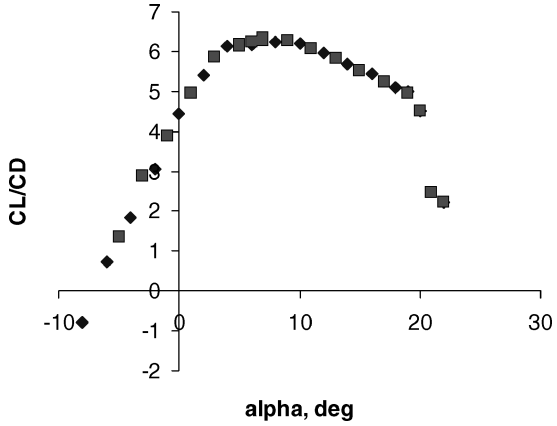

Fig. 7c Lift-to-drag ratio, fins on top at 0.6*b* and 10 deg: ◆, baseline and ■, additional data points.

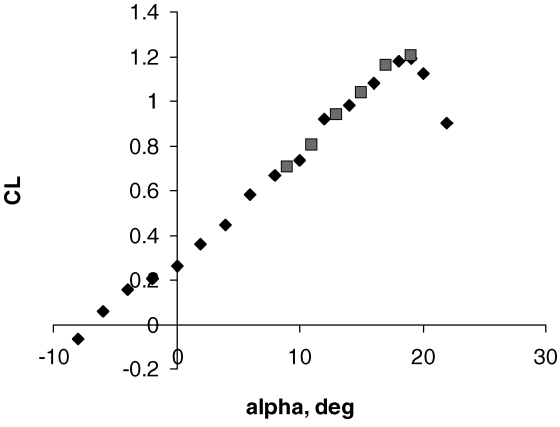

Fig. 8a Lift coefficient of clean wing: ◆, baseline and ■, additional points.

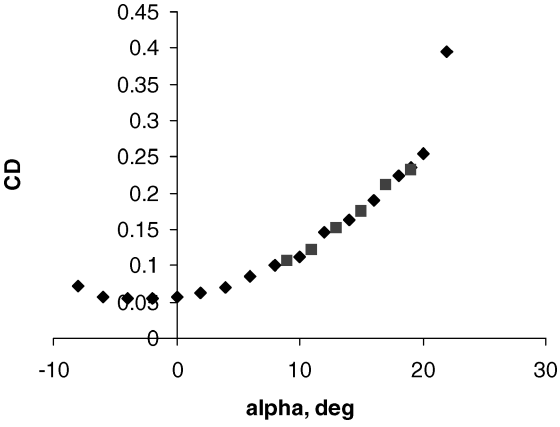

Fig. 8b Drag coefficient of clean wing: ◆, baseline and ■, additional points.

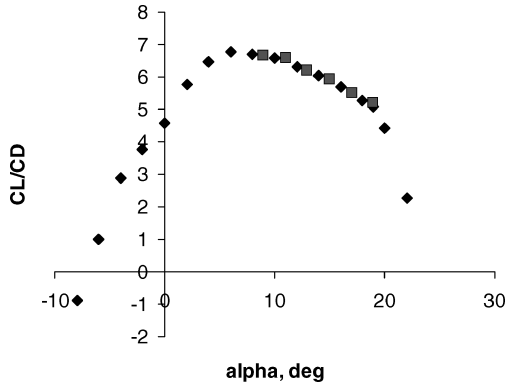

Fig. 8c Aerodynamic efficiency of clean wing: ◆, baseline and ■, additional points.

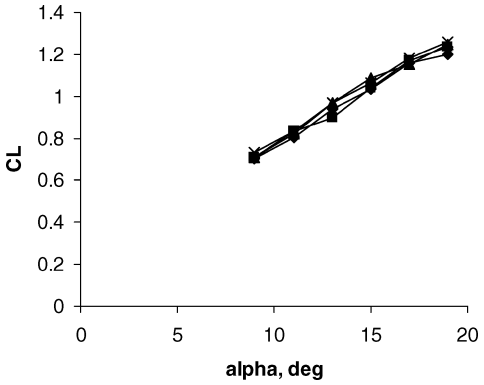

Fig. 9a Effect of fin angle of attack of wing lift coefficient: ◆, clean wing, additional points; ■, fins on top at 0.6*b* and 5 deg; △, fins on top at 0.6*b* and 10 deg; and ×, fins on top at 0.6*b* and 15 deg.

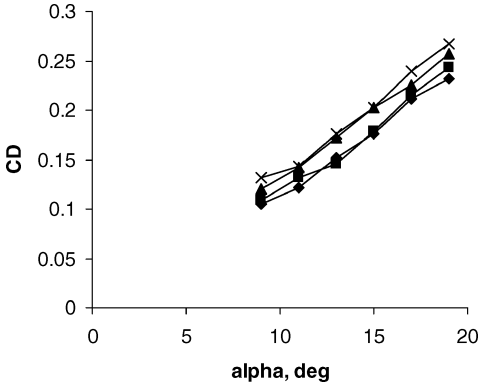

Fig. 9b Effect of fin angle of attack on wing drag coefficient: ◆, clean wing, additional points; ■, fins on top at 0.6*b* and 5 deg; △, fins on top at 0.6*b* and 10 deg; and ×, fins on top at 0.6*b* and 15 deg.

Also, the two values for $\alpha = 7$ deg were very close to each other, whereas the two for $\alpha = 5$ deg coincided. These two series of tests further showed that the tunnel was producing repeatable and reliable results.

To further explore the range of α of the most practical interest for this study, the clean wing configuration was tested at 6 additional values of α, the odd numbered values between 9 and 19 (these two included), thus providing 6 additional data points. These data points were then superimposed onto the original set of data for the wing lift coefficient, drag coefficient, and aerodynamic efficiency, C_L/C_D (Figs. 8a, 8b, and 8c, respectively). The agreement was quite good.

Next, two additional settings for the delta fins were examined. The pivot points for the fins were kept at $y = \pm 0.6s$ and the same chordwise location, $0.66c$, but their angle of attack was set first to 5 deg then 15 deg, which still produced corotating vortices relative to the main wing trailing vortices. The wing angle of attack for this series of tests was varied from 9 to 19 deg, odd-numbered whole degrees. The results of these tests are summarized in Figs. 9a–9c and show the effects of the fins set this way on the wing lift coefficient, drag coefficient, and C_L/C_D, respectively. The points corresponding to the clean wing and the wing with fins at $\alpha_F = 10$ deg are also included for comparison. Note that the lowest of the three setting, that is, $\alpha_F = 5$ deg, produced only minor changes in the wing characteristics, probably within the uncertainties of the tunnel. Note that the highest among the three settings, that is, $\alpha_F = 15$ deg, caused a lower increase in lift but a higher increase in drag than $\alpha_F = 10$ deg. Therefore, the C_L/C_D suffered from two effects. Note from Figs. 9 that it would be detrimental to change the fin setting from $\alpha_F = 10$ to $\alpha_F = 15$ deg. There might, however, be a value in between that would yield the highest wing aerodynamic efficiency, C_L/C_D. Further tests are necessary to determine if this is the case. Note that the existence of optimal settings will depend on the specific wing/fin combination.

For the next phase of the study, the fins were moved inboard to the points at $y = \pm 0.5s$, which is the lower limit of the optimal range for trailing vortex alleviation.[1,2] The chordwise location remained at $0.66c$, and the fin setting at $\alpha_F = 10$ deg. The results are shown in Figs. 10a, 10b, and 10c, and show C_L, C_D, and C_L/C_D, respectively,

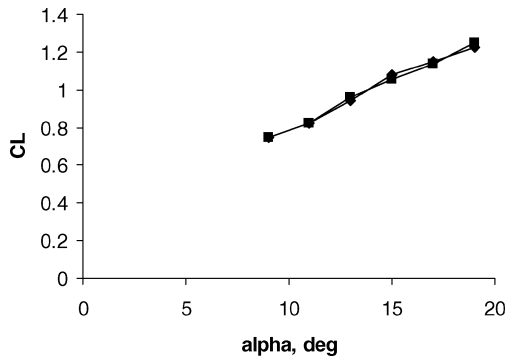

Fig. 10a Effect of fin spanwise location on wing lift coefficient: ◆, fins on top at 0.6*b* and 10 deg and ■, fins on top at 0.5*b* and 10 deg.

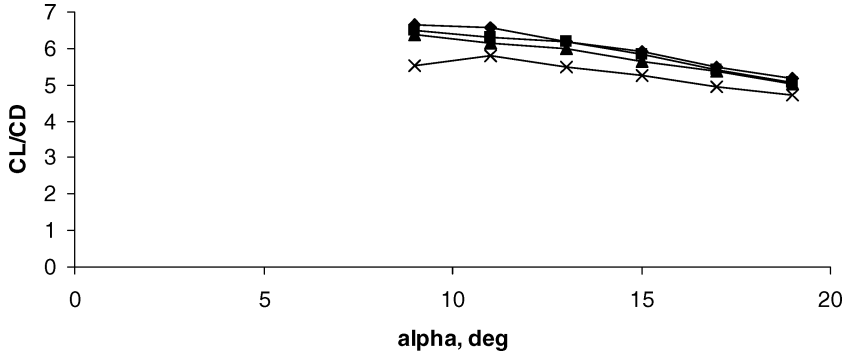

Fig. 9c Effect of fin angle of attack on wing aerodynamic efficiency: ◆, clean wing, additional points; ■, fins on top at 0.6*b* and 5 deg; △, fins on top at 0.6*b* and 10 deg; and ×, fins on top at 0.6*b* and 15 deg.

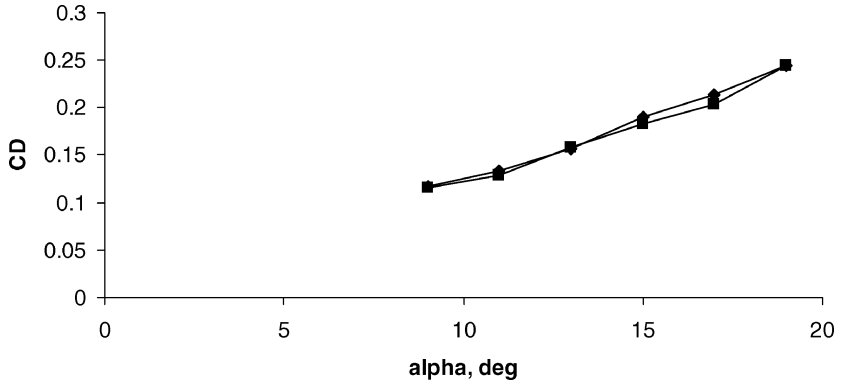

Fig. 10b Effect of fin spanwise location on wing drag coefficient: ◆, fins on top at 0.6*b* and 10 deg and ■, fins on top at 0.5*b* and 10 deg.

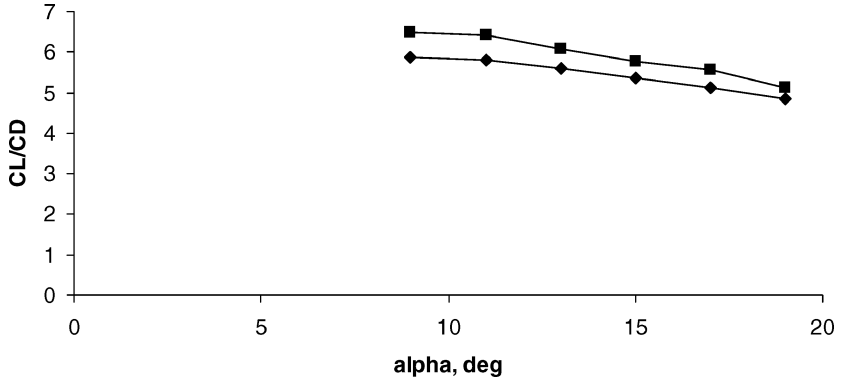

Fig. 10c Effect of fin spanwise location on wing aerodynamic efficiency: ◆, fins on top at 0.6*b* and 10 deg and ■, fins on top at 0.5*b* and 10 deg.

as functions of α. The data points for $y = \pm 0.6s$ are added for comparison. Note that due to this change both the wing lift and drag decrease, with the drag decrease being more pronounced so that the C_L/C_D improves.

Note that no attempt has been made during this preliminary study to optimize the fin geometry. This issue warrants a more detailed examination. From the standpoint of trailing vortex instability acceleration, it is irrelevant whether the fins are on the top or bottom surface of the wing. Because they will still add to the downwash and act as fences, the effects of bottom-mounted fins should be studied. Still another reason for looking into this arrangement is the attractiveness of the solution from the overall system design standpoint: If the fins were found to work well on the bottom surface, then it might be possible to use landing gear doors for this purpose, which would be a great weight advantage.

Uncertainties

The following are the estimates of the uncertainty levels associated with all of the variables involved in this investigation.

The angle of attack of the main wing could be determined to within ± 0.2 deg. The angle of attack of the delta fins is accurate to within ± 0.5 deg. Whereas the wing angle of attack was set and read via the decal-plug assembly described earlier, the fin angles were measured using a standard-type protractor. All of the lengths could be considered reliable to within 0.5 mm (0.02 in.). The dynamic pressure uncertainty is estimated to be ± 0.1 kPa (2.1 psf). Finally, the lift and drag force readouts are estimated to be reliable to within ± 0.04 N (0.01lb).

Conclusions

A preliminary investigation into the effects of discrete midspan vortex injection on the performance of a rectangular wing model has been conducted in a wind tunnel. The vortices were injected via a pair of movable delta fins attached to the upper surface of the wing at a single spanwise position, two spanwise locations, and three different angles of attack of the fins. The injected vortices consistently altered the flow pattern around the wing and, thus, its aerodynamic characteristics. Although the wing with attached fins produced larger drag values, it also generated a noticeable increase in lift acting as a vortex flap, or a fin flap, of a kind. For the particular geometry of the fins employed in the study, these changes depended on both the fin angles of attack and their spanwise location. Even when considered apart from the accompanying lift increases, the measured drag increases are not of such extent to disqualify from further studies this method for trailing vortex alleviation. When the lift enhancements are included, the scheme becomes very attractive. It has been shown that when the fins are at 60% of the semispan, injection with fin angle of attack of 10 deg is more beneficial than with either 5 or 15 deg. Moving the fin pivot point location from 60 to 50% of the semispan produced lower both lift and drag increases over the clean wing configuration so that the aerodynamic efficiency of the wing improved consistently over the wing angle-of-attack range investigated. Although this preliminary study has included two spanwise locations as well as three fin angles of attack, no attempt was made to optimize the delta fin geometry. This aspect of the study warrants a detailed investigation. Also other spanwise locations between 50 and 60% of the semispan should be tested, as well as configurations with the fins attached to the underside of the wing.

References

[1]Nikolic, V. R., and Jumper, E. J., "Attenuation of Airplane Wake Vortices by Excitation of Far-Field Instability," AIAA Paper 93-3511, Aug. 1993.

[2]Nikolic, V. R., "A Study of the Development and Attenuation of Wing-Generated, Vortical Wakes," Ph.D. Dissertation, Dept. of Aerospace and Mechanical Engineering, Univ. of Notre Dame, Notre Dame, IN, March 1993.

[3]Rossow, V. J., "Lift-Generated Vortex Wakes of Subsonic Aircraft," *Progress in Aerospace Sciences*, Vol. 35, 1999, pp. 507–660.

[4]Rossow, V. J., "Prospects for Alleviation of Hazard Posed by Lift-Generated Wakes," *Proceedings of the Aircraft Wake Vortices Conference*, Vol. 1, Federal Aviation Administration, Rept. DOT/FAA/SD-92/1.1, DOT-VNTSC-FAA-92-7.1, Dept. of Transportation, Washington, DC, 29–31 Oct. 1991, p. 22-1–22-40.

[5]Abbot, I. H., and von Doenhoff, A. E., *Theory of Wing Sections*, Dover, New York, 1959, pp. 488–489.

[6]Barlow, J. B., Rae, W. H., Jr., and Pope, A., *Low-Speed Wind Tunnel Testing*, 3rd ed., Wiley, New York, 1999, p. 227.